JOC Article

# Bottom-Up Synthesis of Optically Active Oligonaphthalenes: Three Different Pathways for Controlling Axial Chirality[1]

Kazunori Tsubaki,*,† Hiroyuki Tanaka,† Kazuto Takaishi,† Masaya Miura,† Hiroshi Morikawa,† Takumi Furuta,‡ Kiyoshi Tanaka,‡ Kaoru Fuji,§ Takahiro Sasamori,† Norihiro Tokitoh,† and Takeo Kawabata†

*Institute for Chemical Research, Kyoto University, Gokasho, Uji, Kyoto, 611-0011, Japan, School of Pharmaceutical Sciences, University of Shizuoka, Yada, Shizuoka, 422-8002, Japan, and Faculty of Pharmaceutical Sciences, Hiroshima International University, 5-1-1 Hirokoshingai, Kure, Hiroshima, 737-0112, Japan*

*tsubaki@fos.kuicr.kyoto-u.ac.jp*

*Received May 10, 2006*

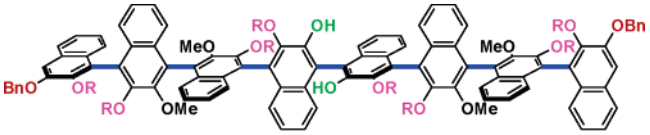


The oxidative homocoupling of optically active binaphthalenes **1a**−**d** with a stoichiometric amount of $CuCl_2$ and amines afforded quaternaphthalenes **2a**−**d** in up to 93% de. The high diastereoselectivities were achieved through three different pathways (epimerization of the axis together with diastereoselective crystallization, thermodynamic, and kinetic control pathways). The type of side chains on the naphthalene influenced which pathway dominates. Three pathways were applicable to octinaphthalenes (**8a**−**d**) and hexadecanaphthalene **10a** with 46−99% de. The absolute configuration of the newly formed axial bond was determined by (1) X-ray crystallographic analysis, (2) transformation to known compounds **15** and **16**, (3) CD spectra of oligonaphthalenes with two pyrene rings as exciton parts, and (4) the shift values in $^{13}C$ NMR spectra of $^{13}C$-enriched derivatives **29**−**31** toward chiral shift reagent Eu(+tfc)$_3$.

## Introduction

Helical motifs such as DNA double helices and various helices in peptide secondary structures are among the most ordered structures found in nature. These natural helical motifs have inspired supramolecular chemists to construct various types of artificial helical molecules.[2] These artificial helical molecules can be broadly classified into two groups. One is static and/or stable helical molecules,[3] which are represented by helicene derivatives, and the other is dynamic helical molecules, which are constructed by the addition of promoter molecules such as metal cations,[4] optically active small molecules,[5] and gelators.[6] However, the former group has inherent synthetic difficulties against the selective introduction of functional groups on their periphery, while the latter only maintains the helical structure under limited conditions.

Meanwhile, the precise, bottom-up construction of molecules from a nano to several tens of nanometer scale is one of most challenging fields in chemistry. Although several molecules have

† Kyoto University.
‡ University of Shizuoka.
§ Hiroshima International University.

(1) A preliminary communication of part of this work has been published: Tsubaki, K.; Miura, M.; Morikawa, H.; Tanaka, H.; Kawabata, T.; Furuta, T.; Tanaka, K.; Fuji, K. *J. Am. Chem. Soc*. **2003**, *125*, 16200−16201.

(2) For recent reviews: (a) Nakano, T.; Okamoto, Y. *Chem. Rev*. **2001**, *101*, 4013−4038. (b) Schmuck, C. *Angew. Chem., Int. Ed*. **2003**, *42*, 2448−2452. (c) Chow, H.-F.; Wan, C.-W. *J. Org. Chem*. **2001**, *66*, 5042−5047. (d) Sugimura, T.; Kurita, S.; Inoue, S.; Fujita, M.; Okuyama, T.; Tai, A. *Enantiomer* **2001**, *6*, 35−42. (e) Ma, L.; White, P. S.; Lin, W. *J. Org. Chem*. **2002**, *67*, 7577−7586. (f) Hattori, T.; Iwato, H.; Natori, K.; Miyano, S. *Tetrahedron: Asymmetry* **2004**, *15*, 881−887. (g) Shibata, T.; Tsuchikama, K. *Chem. Commun*. **2005**, 6017−6019.

(3) (a) Kiupel, B.; Niederalt, C.; Nieger, M.; Grimme, S.; Vögtle, F. *Angew. Chem., Int. Ed*. **1998**, *37*, 3031−3034. (b) Takata, T.; Furusho, Y.; Murakawa, K.; Endo, T.; Matsuoka, H.; Hirasa, T.; Matsuo, J.; Sisido, M. *J. Am. Chem. Soc*. **1998**, *120*, 4530−4531. (c) Jiang, H.; Léger, J.-M.; Huc, I. *J. Am. Chem. Soc*. **2003**, *125*, 3448−3449. (d) Aoki, T.; Kaneko, T.; Maruyama, N.; Sumi, A.; Takahashi, M.; Sato, T.; Teraguchi, M. *J. Am. Chem. Soc*. **2003**, *125*, 6346−6347.

(4) (a) Hasenknopf, B.; Lehn, J.-M.; Baum, G.; Fenske, D. *Proc. Natl. Acad. Sci. U.S.A*. **1996**, *93*, 1397−1400. (b) Albrecht, M. *Chem. Rev*. **2001**, *101*, 3457−3498. (c) Cui, Y.; Lee, S. J.; Lin, W. *J. Am. Chem. Soc*. **2003**, *125*, 6014−6015.

(5) Nonokawa, R.; Yashima, E. *J. Am. Chem. Soc*. **2003**, *125*, 1278−1283.

(6) Goto, H.; Zhang, H. Q.; Yashima, E. *J. Am. Chem. Soc*. **2003**, *125*, 2516−2523.

10.1021/jo060974v CCC: $33.50 
Published on Web 07/26/2006

been recently reported, each is comprised of aryl rings that are directly connected to each other.[7] Hence, completely controlling the number of aryl rings, axial chirality, and the type and/or arrangement of the functional groups on the aryl rings are difficult tasks. We have investigated optically active rod-shaped oligo(2,3-dioxyfunctionalized)naphthalenes, which are connected at the 1,4-positions in a copper-promoted oxidative homocoupling reaction.[8] Important characteristics of these oligonaphthalenes are: (1) a rigid framework in the rod direction, (2) around the axes, they have chirality and some degree of flexibility, and (3) functional groups can be introduced into scaffolding 2,3-dioxy groups. In constructing optically active oligonaphthalenes, the toughest synthetic difficulty is forming axial bonds with high optical purity. Although optically active naphthalene derivatives have been used as substrates, previous papers have reported that in a homocoupling reaction, the corresponding dimers were obtained with low diastereoselectivities (~10% de).[8b,d,9a] Thus, effective chirality induction from the optically active axis to the newly formed axis did not occur. To overcome this low diastereoselectivity, Okamoto and Habaue applied a catalytic amount of copper(I) and a chiral diamine combination, which gave an excellent enantiomeric excess of the coupling of 2-naphthols toward polymerization of the chiral binaphthalene as a monomer unit.[9] They obtained quaternaphthalene with a 64% de in the dimerization of a chiral binaphthalene derivative.[9a] We have also been investigating the synthesis of optically active oligonaphthalenes. In this paper, we report the asymmetric synthesis of optically active oligonaphthalenes through three different pathways, which depend on the variations of the naphthalene side chains.

## Results and Discussion

**Synthesis of the Quaternaphthalenes from Homocoupling of Optically Active Binaphthalenes.** Diastereoselectivities were investigated using optically active binaphthalenes **1a**−**d**,[10] which possessed several types of side chains, under copper(II)-promoted oxidative coupling conditions (Scheme 1 and Table 1).

Table 1 overviews the results. Moderate to good diastereoselectivities were observed under the appropriate combination of substrate and amine. In the early stage of our studies, we tried to explain these diastereoselectivities by a single pathway. However, we noticed that a large amount of brown precipitate was generated only when (*S*)-1-phenylethylamine (**3**) and (*S*)-**1a**, which have a methoxy group on naphthalene (Table 1, entry 3), were combined. This led us to consider that there was more than one pathway triggering these diastereoselectivities.

For (*S*)-**1a** (entries 1−5), diastereoselectivity (12% de) was barely observed using (*RS*)- or (*R*)-1-phenylethylamine (**3**), whereas (*S*)-**3** gave a high selectivity (75% de) and a brown precipitate (entries 1, 2 vs 3). Brussee,[11] Kočovský,[12] and Wulff[13] have reported that copper- and amine-mediated deracemization of binol derivatives together with diastereoselective crystallization afforded chiral binol in a high enantio excess. To confirm the mechanism of the high de for (*S*)-**1a** and (*S*)-**3**, the brown precipitate was removed by filtration. Next, the precipitate and the filtrate were separately purified (entries 4 and 5). An extremely high diastereoselectivity was observed from the precipitate (93% de, 58% yield), but the filtrate gave a low selectivity (17% de, 15% yield). Furthermore, the same

**SCHEME 1. Oxidative Coupling of Binaphthalenes 1a−d**

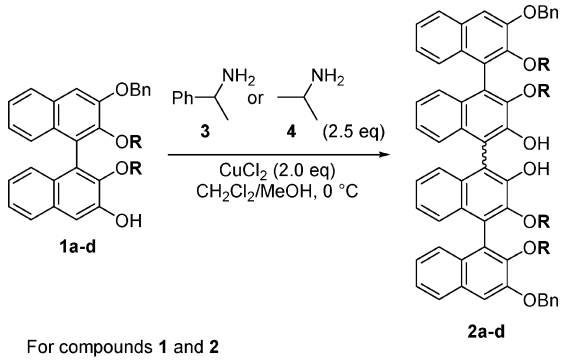


For compounds **1** and **2**
**a**: R = Me, **b**: R = $CH_2CO_2t$-Bu, **c**: R = $CH_2CON(Et)_2$, **d**: R = *n*-Bu

**TABLE 1. Oxidative Coupling of Binaphthalenes 1a−d**

| entry | substrate | amine | major isomer[a] | isolation[b] | yield (%)[c] | de (%)[d] |
|---|---|---|---|---|---|---|
| 1 | (*S*)-**1a** | (*RS*)-**3** | (*S*,*S*,*S*)-**2a** | − | 73 | 12 |
| 2 | | (*R*)-**3** | | − | 69 | 26 |
| 3 | | (*S*)-**3** | | PF | 87 | 75 |
| 4 | | (*S*)-**3** | | P | 58 | 93 |
| 5 | | (*S*)-**3** | | F | 15 | 17 |
| 6 | (*S*)-**1b** | (*R*)-**3** | (*S*,*S*,*S*)-**2b** | − | 77 | 82 |
| 7 | (*R*)-**1b** | (*RS*)-**3** | (*R*,*R*,*R*)-**2b** | − | 54 | 79 |
| 8[e] | | (*R*)-**3** | | − | 75 | 19 |
| 9 | | **4** | | − | 55 | 62 |
| 10 | (*S*)-**1c** | (*RS*)-**3** | (*S*,*S*,*S*)-**2c** | − | 96 | 75 |
| 11 | | (*R*)-**3** | | − | 81 | 75 |
| 12 | | (*S*)-**3** | | − | 89 | 70 |
| 13 | | **4** | | − | 94 | 81 |
| 14 | (*S*)-**1d** | (*S*)-**3** | (*S*,*S*,*S*)-**2d** | − | 77 | 62 |
| 15 | | (*RS*)-**3** | | − | 77 | 65 |

[a] Absolute configuration of major isomer was determined by transformation to the known compound or an X-ray analysis. See text. [b] − = no precipitation; PF = without separation of precipitate and filtrate; P = from precipitate; F = from filtrate. [c] Isolated yield. [d] Based on the isolated yields of corresponding diastereomers. [e] Reaction temperature = 0 °C to rt.

(7) (a) Pu, L. *Chem. Rev*. **1998**, *98*, 2405−2494. (b) Inoue, S.; Nakanishi, H.; Takimiya, K.; Aso, Y.; Otsubo, T. *Synth. Met*. **1997**, *84*, 341−342. (c) Yamaguchi, S.; Goto, T.; Tamao, K. *Angew. Chem., Int. Ed*. **2000**, *39*, 1695−1697. (d) Meier, H.; Hormaza, A. *Eur. J. Org. Chem*. **2003**, 3372−3377. (e) Izumi, T.; Kobashi, S.; Takimiya, K.; Aso, Y.; Otsubo, T. *J. Am. Chem. Soc*. **2003**, *125*, 5286−5287. (f) Miyata, Y.; Nishinaga, T.; Komatsu, K. *J. Org. Chem*. **2005**, *70*, 1147−1153.

(8) (a) Tanaka, K.; Furuta, T.; Fuji, K.; Miwa, Y.; Taga, T. *Tetrahedron: Asymmetry* **1996**, *7*, 2199−2202. (b) Fuji, K.; Furuta, T.; Tanaka, K. *Org. Lett*. **2001**, *3*, 169−171. (c) Tsubaki, K.; Tanaka, H.; Furuta, T.; Tanaka, K.; Kinoshita, T.; Fuji, K. *Tetrahedron* **2002**, *58*, 5611−5617. (d) Furuta, T.; Tanaka, K.; Tsubaki, K.; Fuji, K. *Tetrahedron* **2004**, *60*, 4431−4441. (e) Pieraccini, S.; Ferrarini, A.; Fuji, K.; Gottarelli, G.; Lena, S.; Tsubaki, K.; Spada, G. P. *Chem.-Eur. J*. **2006**, *12*, 1121−1126. (f) Tsubaki, K.; Miura, M.; Nakamura, A.; Kawabata, T. *Tetrahedron Lett.* **2006**, *47*, 1241−1244. (g) Tsubaki, K.; Takaishi, K.; Tanaka, H.; Miura, M.; Kawabata, T. *Org. Lett*. **2006**, *8*, 2587−2590.

(9) (a) Habaue, S.; Seko, T.; Okamoto, Y. *Macromolecules* **2002**, *35*, 2437−2439. (b) Habaue, S.; Seko, T.; Okamoto, Y. *Macromolecules* **2003**, *36*, 2604−2608. (c) Habaue, S.; Seko, T.; Isonaga, M.; Ajiro, H.; Okamoto, Y. *Polym. J.* **2003**, *35*, 592−597. (d) Habaue, S.; Ajiro, H.; Yoshii, Y.; Hirasa, T. *J. Polym. Sci., Part A: Polym. Chem.* **2004**, *42*, 4528−4534. (e) Habaue, S.; Muraoka, R.; Aikawa, A.; Murakami, S.; Higashimura, H. *J. Polym. Sci., Part A: Polym. Chem*. **2005**, *43*, 1635−1640. (f) Temma, T.; Habaue, S. *Tetrahedron Lett.* **2005**, *46*, 5655−5657. (g) Habaue, S.; Ishikawa, K. *Polym. Bull*. **2005**, *55*, 243−250.

(10) The optically active binaphthalenes **1a**−**d** were synthesized from the corresponding dibenzyl derivatives (Supporting Information).

(11) (a) Brussee, J.; Jansen, A. C. A. *Tetrahedron Lett*. **1983**, *24*, 3261−3262. (b) Brussee, J.; Groenendijk, J. L. G.; te Koppele, J. M.; Jansen, A. C. A. *Tetrahedron* **1985**, *41*, 3313−3319.

(12) (a) Smrčina, M.; Lorenc, M.; Hanuš, V.; Sedmera, P.; Kočovský, P. *J. Org. Chem*. **1992**, *57*, 1917−1920. (b) Smrčina, M.; Poláková, J.; Vyskočil, S.; Kočovský, P. *J. Org. Chem*. **1993**, *58*, 4534−4538.

(13) Zhang, Y.; Yeung, S.-M.; Wu, H.; Heller, D. P.; Wu, C.; Wulff, W. D. *Org. Lett*. **2003**, *5*, 1813−1816.

diastereomer (*S*,*S*,*S*)-**2a** was preferentially obtained from both the precipitate and the filtrate. These results indicate that the origin for the axial chirality control should be epimerization of the axis together with diastereoselective crystallization.[14]

For other substrates **1b**−**d** (entries 6−15), a precipitate was not observed and homochiral quaternaphthalenes were predominantly formed over heterochiral quaternaphthalenes with a 19−82% de. Thus, axial chirality was not induced via epimerization together with diastereoselective crystallization. When **1b**, which had two *tert*-butoxycarbonyl methyl groups, was used as starting material, **2b** was obtained with a high selectivity (ca. 80% de) regardless of the chirality of 1-phenylethylamine (**3**) (entries 6 and 7). This chirality induction was sensitive to the reaction temperature; the diastereoselectivity drastically decreased from about 80% to 19% de as the temperature increased (entries 6, 7 vs 8). Moreover, it should be emphasized that a moderate selectivity (62% de) was observed in the presence of achiral isopropylamine (**4**) (entry 9). Because the axial chirality of **1b** was the sole chiral source in the reactions, the origin of chirality induction was a chirality transfer from the optically active axis to the newly formed axis. The effects of *tert*-butoxycarbonyl methyl on the side chain were similar to the case for homocoupling of 3-hydroxy-2-naphthoates reported by Nakajima[15] and Kozlowski.[16] They noted that the coordination of the carbonyl to copper was crucial for a high enantioselectivity. However, substrates with an amide group **1c**, which might generate a tight coordination to copper, showed slightly lower selectivities than those of **1b** (entries 10−12). To our surprise, **1d** gave a relatively high selectivity (62−65% de) by appending to the noncoordinating *n*-butyl group (entries 14 and 15).

To elucidate the reasons for the diastereoselectivities, the time course for the conversion and diastereoselectivities of the corresponding coupling reactions of **1b**−**d** (Figure 1a, c, and e) as well as epimerization between the homochiral and heterochiral products **2b**−**d** under the coupling reaction conditions (Figure 1b, d, and f) were monitored. The data revealed that chirality was induced by two or more pathways, which depend on the side chains.

In the coupling reaction of (*S*)-**1d**, the diastereoselectivity of (*S*,*S*,*S*)-**2d** increased from 54% de (5 min) and plateaued at 68% de after 4 h (Figure 1a). Furthermore, the epimerization reactions, which began from (*S*,*S*,*S*)- and (*S*,*R*,*S*)-**2d**, also reached equilibrium at 70% de (Figure 1b). A similar tendency was observed in the coupling reaction of (*R*)-**1b** and epimerization of **2b** (Figure 1c and d).[17] The data indicated that the

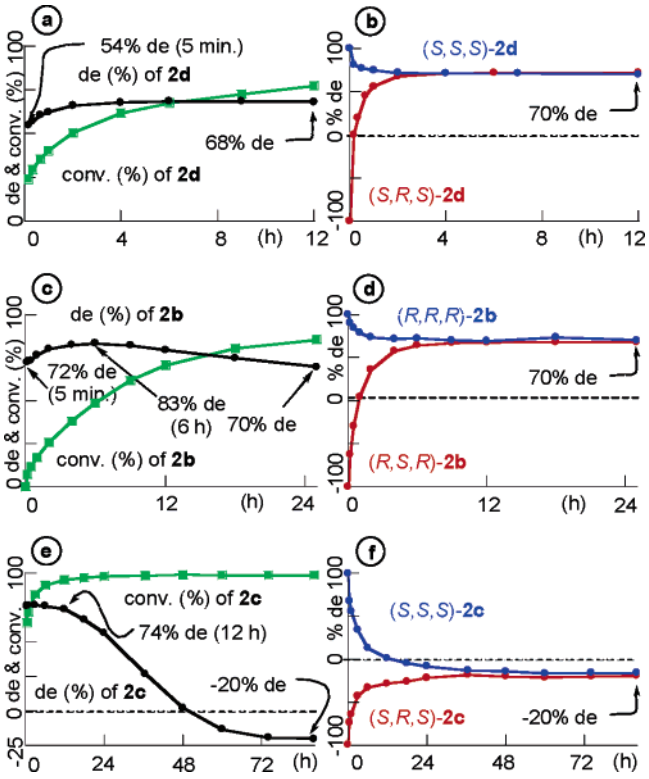


**FIGURE 1.** Time course of the diastereoselectivities with the coupling reaction (a, c, and e) and with epimerization (b, d, and f). Reaction conditions: For the homocoupling reaction, **1b**−**d** (0.2 mmol), $CuCl_2$ (0.4 mmol), (*R*,*S*)-**3** (0.5 mmol), MeOH/$CH_2Cl_2$ = 1 mL/1 mL, 0 °C. For epimerization, **2b**−**d** (0.1 mmol), $CuCl_2$ (0.4 mmol), (*R*,*S*)-**3** (0.5 mmol), MeOH/$CH_2Cl_2$ = 1 mL/1 mL, 0 °C. Conversion and de were monitored and determined by HPLC (cosmosil-packed column 5SL-2, (nacalai), hexane/chloroform/ethyl acetate = 92/6/2, 2.0 mL/min for **2d**, hexane/chloroform/ethyl acetate = 90/5/5, 1.2 mL/min for **2b**, hexane/ethanol = 90/10, 1.0 mL/min for **2c**).

axial chirality should be controlled by the difference in the thermodynamic stabilities of the diastereomeric product/copper adducts. On the other hand, the pathway of coupling reactions of (*S*)-**1c** and the epimerization of **2c** were completely different from those of the former two cases. The initial diastereoselectivity of the coupling reaction of (*S*)-**1c** was about 75% de, which remained around 75% de for 12 h. The diastereoselectivity then gradually decreased and plateaued at −20% de after 72 h. Both diastereomers slowly underwent epimerization and achieved equilibrium at −20% de after 36 h (Figure 1e and f). Thus, the rapid coupling reaction with a high diastereoselectivity and a slow epimerization of the newly formed axial bond led to a product under kinetic control.

Epimerization was due to either a rotation around the axial bond or cleavage and regeneration of the axial bond. Thus, a crossover experiment was conducted to determine the cause of epimerization (Scheme 2).

A 1:1 mixture of (*S*,*S*,*S*)-**2c** and (*S*,*S*,*S*)-**2c**-$d_{14}$ with two deuterated benzyl groups on the top and bottom naphthalenes was treated under coupling conditions, and the degree of epimerization of the central axial bond was monitored by HPLC. After the epimerization reached equilibrium (−20% de, see Figure 1f), the mass distribution was measured by FAB mass spectrometry (Figure 2). Because scrambled mass ion peaks derived from **2c**-$d_7$ were not observed, epimerization occurs by axial bond rotation. On the basis of these results, we propose

(14) Neither precipitation nor enantioselectivity was observed for self-coupling of 3-benzyloxy-naphthalen-2-ol under $CuCl_2$ and (*S*)-1-phenylethylamine.

(15) (a) Noji, M.; Nakajima, M.; Koga, K. *Tetrahedron Lett.* **1994**, *35*, 7983−7984. (b) Nakajima, M.; Kanayama, K.; Miyoshi, I.; Hashimoto, S. *Tetrahedron Lett.* **1995**, *36*, 9519−9520. (c) Nakajima, M.; Miyoshi, I.; Kanayama, K.; Hashimoto, S.; Noji, M.; Koga, K. *J. Org. Chem.* **1999**, *64*, 2264−2271.

(16) (a) Li, X.; Yang, J.; Kozlowski, M. C. *Org. Lett.* **2001**, *3*, 1137−1140. (b) Li, X.; Hewgley, J. B.; Mulrooney, C. A.; Yang, J.; Kozlowski, M. C. *J. Org. Chem.* **2003**, *68*, 5500−5511. (c) Xie, X.; Phuan, P.-W.; Kozlowski, M. C. *Angew. Chem., Int. Ed.* **2003**, *42*, 2168−2170. (d) Mulrooney, C. A.; Li, X.; DiVirgilio, E. S.; Kozlowski, M. C. *J. Am. Chem. Soc.* **2003**, *125*, 6856−6857.

(17) In Figure 4, we proposed homo-dimerization of the radical **5**. However, the actual reaction mechanisms will consist of the homo-dimerization of the radical **5**, hetero-dimerization of radical **5**, and starting material. In Figure 1c, the initial diastereoselectivity of the coupling reaction of (*R*)-**2b** was about 72% de, and the de temporarily increased to 82% after 5 h, and then plateaued at 70% de. These phenomena should be reflected in the balance between the homo- and hetero-dimerization.

**SCHEME 2** [a]

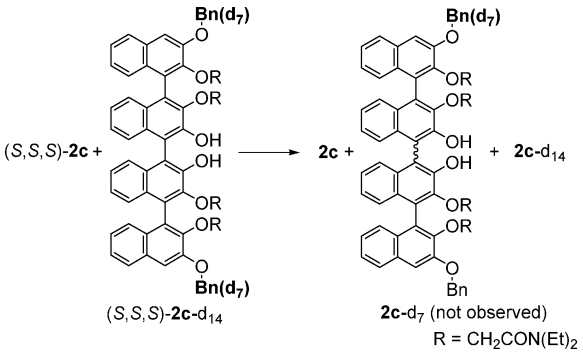


[a] Conditions: (*S*,*S*,*S*)-**2c** (0.5 equiv), (*S*,*S*,*S*)-**2c**-$d_{14}$ (0.5 equiv), $CuCl_2$ (4.0 equiv), (*RS*)-**3** (5.0 equiv), $MeOH/CH_2Cl_2$, 0 °C.

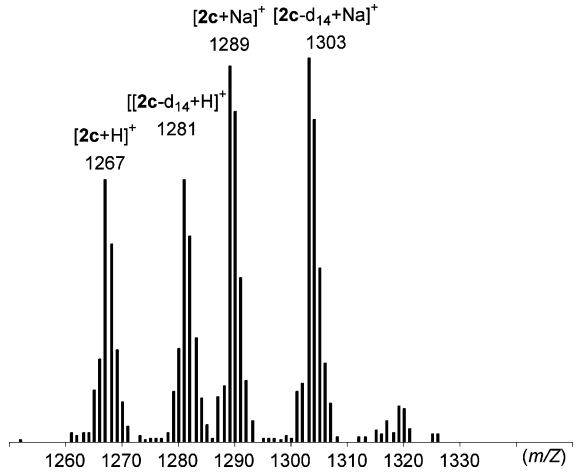


**FIGURE 2.** Mass spectrum of crossover experiment. NBA matrix; ion mode, $FAB^+$; inlet, direct.

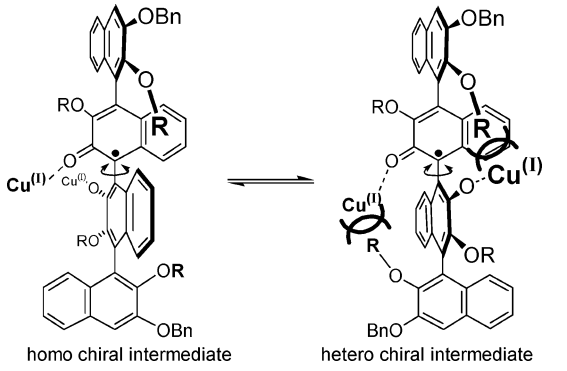


**FIGURE 3.** Proposed mechanism of the epimerization of quaternaphthalenes **2**.

the following model for the thermodynamic stabilities of the diastereomeric intermediates of quaternaphthalenes (Figure 3).

After the coupling reaction, an aryl radical intermediate was generated in the presence of an excess amount of $CuCl_2$, and epimerization of the axial bond occurred through the intermediate. Considering the steric repulsions between the OR groups on the top and bottom of naphthalene rings and Cu (draping amine molecules and/or solvents as ligands) on third and second of naphthalenes rings, a homochiral intermediate is more stable than a heterochiral intermediate. In the case of **2c**, two amide carbonyls tightly coordinated to copper prevail over the steric repulsions between them.

With respect to the diastereoselectivity of the coupling reaction, the following model is proposed (Figure 4).[17] A one-electron oxidation with Cu(II) generates an organic radical, which has the shape speculated as **5**. Thus, to avoid steric repulsion, the OR group on the top naphthalene is oriented in the opposite direction of the OBn group. This OR group controls the direction of the other OR group on the bottom naphthalene through steric repulsion, and the second OR group influences the direction of Cu(I) coordinated to oxygen (as well as the draping amine molecules and/or solvents as ligands).[18] At last, the homocoupling reaction occurs from their opposite face of the Cu(I) site to afford intermediate **6**. Finally, stereochemistry is established through keto−enol tautomerization where the direction of rotation is with the hydrogens on *peri* position passing each other.

**Synthesis of High-Order Naphthalenes.** Next, we investigated the applicability of the three pathways (epimerization of the axis together with diastereoselective crystallization, and axial chirality induction through thermodynamic and kinetic control) to higher naphthalene derivatives **7a**−**d** and **9a** (Scheme 3). Table 2 shows the results.

The epimerization with diastereoselective crystallization pathway was applicable to the conversion of (*S*,*S*,*S*)-**7a** to (*S*,*S*,*S*,*S*,*S*,*S*,*S*)-**8a** (86% yield, 99% de) and to the conversion of (*S*,*S*,*S*,*S*,*S*,*S*,*S*)-**9a** to all-(*S*)-**10a** (78% yield, 79% de). Because of low solubility, higher oligonaphthalenes were not investigated. The coupling reaction of quaternaphthalenes (*S*,*S*,*S*)-**7b**−**d** through other pathways afforded octinaphthalenes **8b**−**d**, which have different substituents on naphthalenes with a relatively high diastereoselectivity (46−83% de).[19] Because these products have sufficient solubility in organic solvents, they could be used as precursors for starting materials of higher oligonaphthalenes.

**Determination of the Absolute Configuration of Newly Formed Axial Bond.** During these studies, three empirical rules were found. (1) The $R_f$ value on silica gel TLC of the homochiral isomer is larger than that of the opposite chirality-containing isomer. This is probably because the dipole moments of the first and third naphthalenes are parallel to the major axis of the corresponding naphthalene and negate each other in the homochiral isomer. (2) The absolute value of the specific rotation of the homochiral isomer is larger than that of the opposite chirality-containing isomer. (3) The amplitude of the CD spectrum of the homochiral isomer is larger than that of the opposite chirality-containing isomer (see Supporting Information).[8d] Rule no. 3 seems to be widely applicable to these oligonaphthalenes, but the difference of the amplitude between corresponding diastereomers becomes smaller as the number

(18) Ultra-remote stereocontrol by conformational communication was reported. Clayden, J.; Lund, A.; Vallverdú, L.; Hellwell, M. *Nature* **2004**, *431*, 966−971.

(19) Because we afforded starting (*S*)- and (*R*)-3,3-bis(benzyloxy)-1,1-binaphthalene-2,2-diol by resolution of the racemic one[21] and the examined reaction conditions, there is disagreement on chiralities between the major product in Table 1, entries 7−9, and the substrate in Table 2, entry 3.

(20) (a) Harada, N.; Nakanishi, K. *Acc. Chem. Res.* **1972**, *5*, 257−263. (b) Harada, N.; Nakanishi, K. *Circular Dichroic Spectroscopy − Exciton Coupling in Organic Stereochemistry*; University Science Books: Mill Valley, CA, 1983. (c) Berova, N.; Nakanishi, K. In *Circular Dichroism: Principles and Applications*, 2nd ed.; Berova, N., Nakanishi, K., Woody, R. W., Eds.; Wiley-VCH: New York, 2000; pp 337−382. (d) Koslowski, A.; Sreerama, N.; Woody, R. W. In *Circular Dichroism: Principles and Applications*; Berova, N., Nakanishi, K., Harada, N., Eds.; Wiley-VCH: New York, 2000; pp 55−95.

(21) Tsubaki, K.; Morikawa, H.; Tanaka, H.; Fuji, K. *Tetrahedron: Asymmetry* **2003**, *14*, 1393−1396.

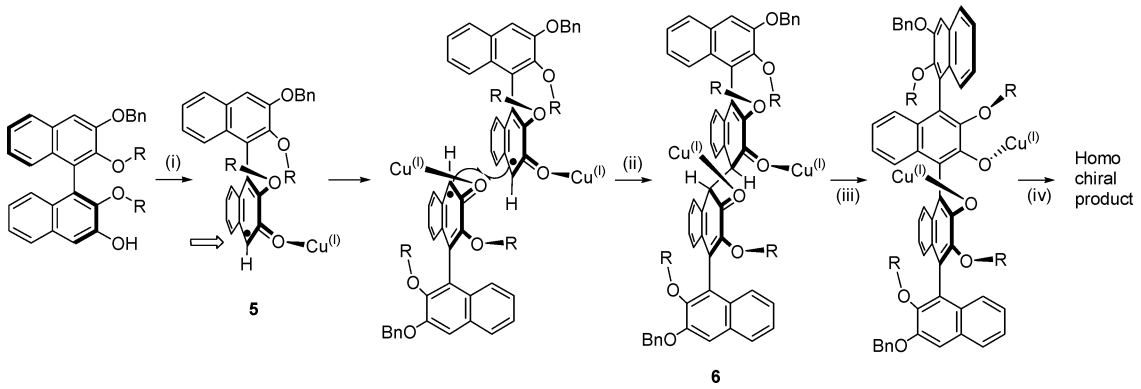


**FIGURE 4.** Proposed mechanism of the dimerization of binaphthols. (i) Cu(II), one-electron oxidation; (ii) coupling; (iii) enolization; (iv) $H^+$.

**SCHEME 3. Oxidative Coupling of Higher Naphthalene Derivatives 7a−d and 9a**

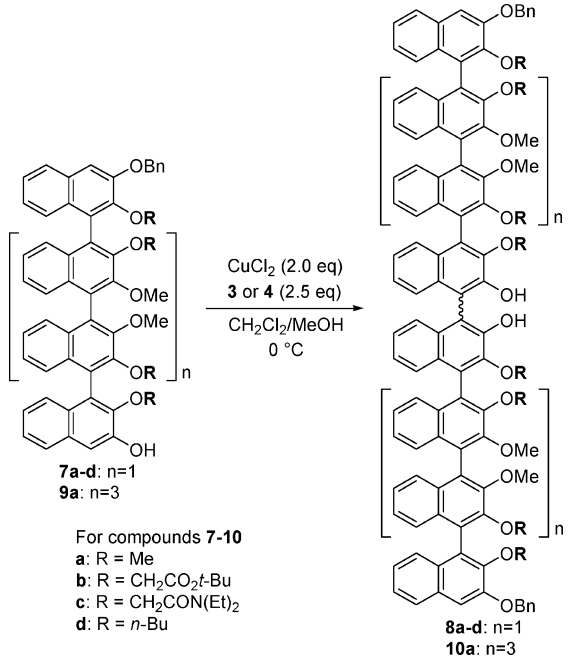


**TABLE 2. Oxidative Coupling of Higher Naphthalene Derivatives 7a−d and 9a**

| entry | substrate | amine | major isomer[a] | yield (%)[b] | de (%)[c,d] |
|---|---|---|---|---|---|
| 1 | (*S*,*S*,*S*)-**7a** | (*S*)-**3** | (*S*,*S*,*S*,*S*,*S*,*S*)-**8a** | 86 | 99 |
| 2 | (*S*,*S*,*S*,*S*,*S*,*S*)-**9a** | (*S*)-**3** | all-(*S*)-**10a** | 78 | 79 |
| 3 | (*S*,*S*,*S*)-**7b**[19] | (*RS*)-**3** | (*S*,*S*,*S*,*S*,*S*,*S*)-**8b** | 50 | 80 |
| 4 | (*S*,*S*,*S*)-**7c** | **4** | (*S*,*S*,*S*,*S*,*S*,*S*)-**8c** | 69 | 46 |
| 5 | (*S*,*S*,*S*)-**7d** | (*RS*)-**3** | (*S*,*S*,*S*,*S*,*S*,*S*)-**8d** | 55 | 83 |

[a] The absolute configuration of the major isomer was determined by transforming into a known compound and comparing the amplitude in the CD spectrum of the corresponding diastereomers using the pyrene method or $^{13}C$ method. See text. [b] Isolated yield. [c] Based on the isolated yields of corresponding diastereomers. [d] The reaction conditions were not optimized.

of naphthalene units increases. Therefore, we are trying to construct a widely applicable determination method for oligonaphthalenes.

The absolute configurations of the newly formed axial bonds were determined using several methods. In a previous paper, we reported the synthesis and determination of the axial chirality of quarter-, sexi-, and octinaphthalenes by comparing the products.[8b,d] For example, for octinaphthalenes **12**, the products

**SCHEME 4** [a]

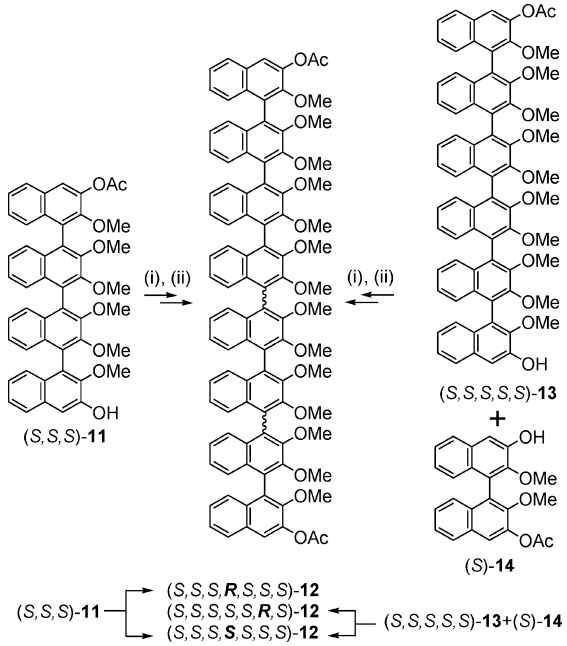


[a] Reaction conditions: (i) $CuCl_2$, (*RS*)-**3**, (ii) MeI, $K_2CO_3$.

of homocoupling of quaternaphthalene (*S*,*S*,*S*)-**11** and those of heterocoupling of sexinaphthalene (*S*,*S*,*S*,*S*,*S*,*S*)-**13** and binaphthalene (*S*)-**14** (Scheme 4) were compared.

Although this comparison method is clear and conclusive for determining the axial chirality, too many reaction steps, especially for oligonaphthalenes with different functional groups on the side chains, are required to determine one unknown axial chirality. Therefore, we used compounds (*S*,*S*,*S*)-**15** and (*S*,*S*,*S*,*S*,*S*,*S*,*S*)-**16**[8b,d] synthesized through the comparison method as the standard materials (Figure 5) and transformed the chirality of unknown compound to these standard materials.

**Determination of the Absolute Configuration of Quaternaphthalenes 2d.** An X-ray crystallographic analysis of major product **2d** derived from (*S*)-**1d** unequivocally defined the structure as (*S*,*S*,*S*) (Figure 6). It is interesting to note that the sum of the dihedral angles of the top and middle axes and the sum of the middle and bottom axes were about 180°. Hence, five naphthalene units are required for a 360° turn.

**Determination of the Absolute Configuration of Quaternaphthalenes 2a−c.** Major diastereomers **2a** and **2b** were

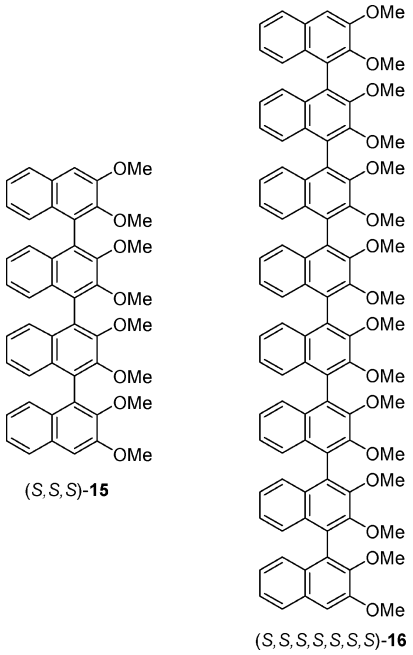


**FIGURE 5.**

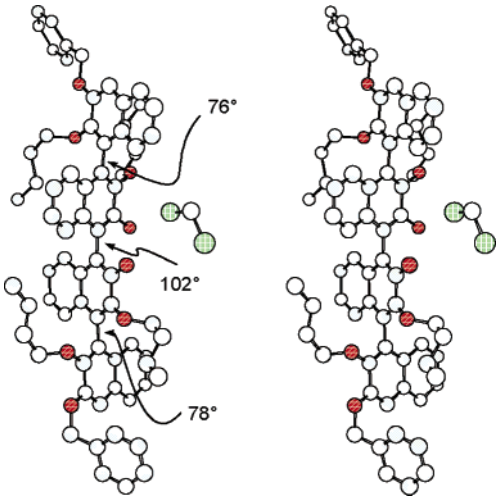


**FIGURE 6.** Stereoview of the crystal structure of (*S*,*S*,*S*)-**2d**. Hydrogen atoms have been omitted for clarity.

converted to standard compound **15** (Scheme 5). Thus, the major diastereomer **2a** derived from (*S*)-**1a** was debenzylated with Pd/C and subsequently four hydroxy groups were methylated to afford all-methoxy derivative **15**, and all of the physical data including the $[\alpha]_D$ value agreed with those of standard (*S*,*S*,*S*)-**15**. Thus, that absolute configuration was determined by the comparison method. The side chains of major diastereomer **2b** derived from (*R*)-**1b** were exhaustively dealkylated by boron tribromide and methylated to give compound **15**, which showed the opposite $[\alpha]_D$ value. Thus, the absolute configuration of major diastereomer **2b** should be determined as (*R*,*R*,*R*). Treatment of (*R*,*R*,*R*)-**2b** with (trimethylsilyl)diazomethane afforded the methyl ether. Next, four *tert*-Bu groups were removed, and diethylamino groups were introduced using BOP to afford (*R*,*R*,*R*)-**17**. On the other hand, major isomer **2d** from (*S*)-**1d** was transformed to **17** and had the same physical data, except an opposite $[\alpha]_D$. Thus, the absolute configuration of the major isomer of **2d** is (*S*,*S*,*S*).

**SCHEME 5**

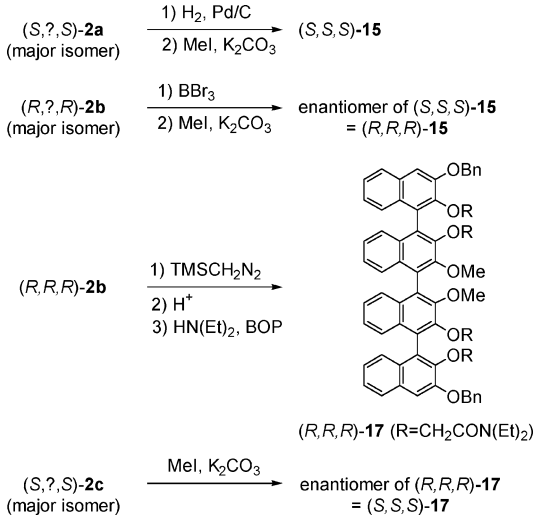


**Determination of the Absolute Configuration of Octi- and Hexadecanaphthalenes 8a−c and 10a.** Major diastereomer **8a**, which was derived from (*S*,*S*,*S*)-**7a**, was converted into octinaphthalene **16** via a route similar to those from **2a** to **15**, in a 31% overall yield in two steps, and the resulting product had data identical to the standard (*S*,*S*,*S*,*S*,*S*,*S*,*S*)-**16**. There is not a standard compound for hexadecanaphthalene **10a**. Therefore, we developed a new and efficient system based on a circular dichroism (CD) exciton chirality method. We focused on the two free hydroxy groups, which stride over the chirality of the unknown axial bond, and chose pyrene as an exciter. Because steric hindrance prohibits the introduction of 2-pyrene carboxylic acid to the scaffolding hydroxy groups, 4-(2-pyreneyl)-butyric acid was selected (Figure 7).

First, the UV spectra and CD spectra of compounds **18**−**20** were carefully examined to determine whether the CD signals derived from the two pyrene parts were separate from those of the oligonaphthalene backbone and whether the CD signals reflect the absolute configuration of the target axial chirality using compounds **18**, **19**, and **21**, which were synthesized from chirality-clear oligonaphthalenes. Figure 8a−c shows the UV and CD spectra. In Figure 8a, the UV−vis spectrum of **21** is the simple sum of the spectrum of the main skeleton **22** and the spectrum (twice as intense) of side chain **26**. The absorption bands at 279, 330, and 346 nm were assigned to the transitions from the pyrene moiety. The mirror image CD spectra of (*R*)- and (*S*)-**21** indicate that the positive or negative sense near 280, 330, and 350 nm reflects the absolute configuration of the target axial bond. Because of the large negative absorption from the quaternaphthalene backbone, the absorption derived from the pyrene groups around 280 nm was buried and that around 330 nm was influenced. However, the sense around 350 nm demonstrated the absolute configuration of the central axial bond (Figure 8b). As shown in Figure 8c, pyrene absorptions around 280 and 330 nm were engulfed by the deep absorption of the octinaphthalene skeleton, and only the absorption at 350 nm survived to indicate the absolute configuration. Considering these results, the absorption around 350 nm on the CD spectra of the major isomer from the homocoupling of (*S*,*S*,*S*,*S*,*S*,*S*,*S*)-**9a** indicates a positive sense. Thus, the target axis is (*S*,*S*,*S*,*S*,*S*,*S*,*S*,*S*,*S*,*S*,*S*,*S*,*S*,*S*).

This pyrene method is applicable for oligonaphthalenes with butyl side chains **2d** and **7d**. Thus, quaternaphthalene **27** derived

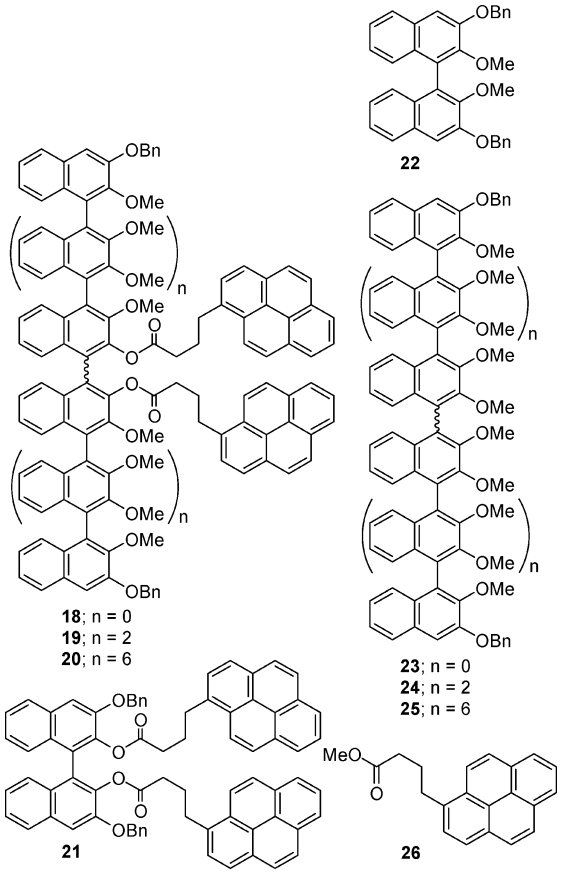


**FIGURE 7.**

from (*S*,*S*,*S*)- and (*S*,*R*,*S*)-**2d**, which have absolute configurations that were determined by the comparison method, indicates a positive sense for (*S*,*S*,*S*) and a negative sense for (*S*,*R*,*S*) near the 350 nm region (Figures 9 and 10). These behaviors are the same for quaternaphthalenes **18** with methoxy side chains. Octinaphthalene **28**, which was derived from the major diastereomer of homocoupling of (*S*,*S*,*S*)-**7d**, shows a positive sense in the 350 nm region. Thus, the target axial chirality should be (*S*,*S*,*S*,*S*,*S*,*S*,*S*).

However, attempts to introduce two pyrenebutyryl groups into the two central hydroxy groups of **2b**, **2c**, **8b**, and **8c** using an acid chloride, an acid anhydride, and various types of condensation reagents (DCC, DIC, EEDQ, and cyanuric chloride) were unfruitful due to the neighboring bulky side chains. Therefore, the absolute configurations of the axial chirality of **8b** and **8c** were determined by comparing the chemical shifts of carbon-13-enriched methyl groups, which were introduced to a series of oligonaphthalenes **29**−**31** after the stepwise addition of europium tris[3-(trifluoromethylhydroxymethylene)-(+) camphorate] [Eu(+tfc)$_3$] (Figures 11 and 12).

When Eu(+tfc)$_3$ was added to (*S*)- and (*R*)-**29** without amide side chains, the shifts of the signals that corresponded to the $^{13}$C-methyl group were negligible. For (*R*,*R*,*R*)- and (*R*,*S*,*R*)-**30**, the absolute configuration was determined on the basis of the comparison and derivation method, and, as the amount of the chiral shift reagent increased relative to **30**, the corresponding $^{13}$C-methyl groups shifted to a lower magnetic field and the degree of the (*R*,*S*,*R*)-**30** shift was larger than that of (*R*,*R*,*R*)-**30**. A similar behavior was detected in octinaphthalenes **31**. Therefore, octinaphthalenes that show a larger lower magnetic

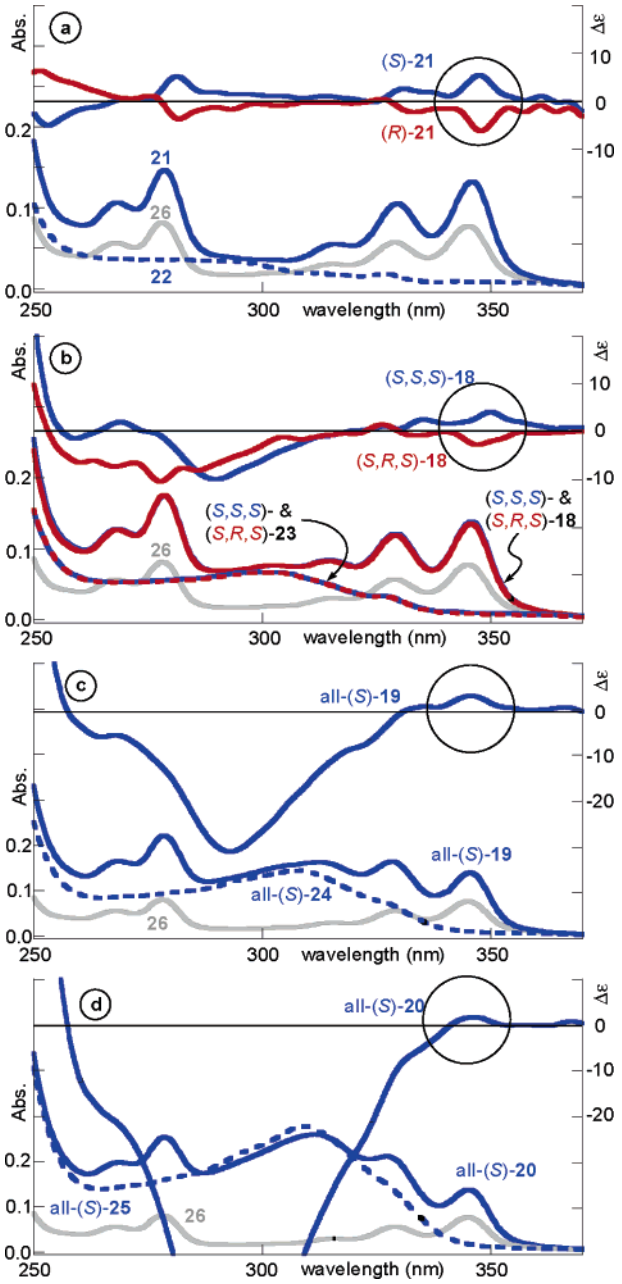


**FIGURE 8.** (a) UV−visible spectra of (*S*)-**22** (dotted blue), **26** (gray), and (*S*)-**21** (blue), and CD spectra of (*S*)-**21** (blue) and (*R*)-**21** (red). (b) UV−visible spectra of (*S*,*S*,*S*)-**23** (dotted blue), (*S*,*R*,*S*)-**23** (dotted red), **26** (gray), (*S*,*S*,*S*)-**18** (blue), and (*S*,*R*,*S*)-**18** (red), and CD spectra of (*S*,*S*,*S*)-**18** (blue) and (*S*,*R*,*S*)-**18** (red). (c) UV−visible spectra of (*S*,*S*,*S*,*S*,*S*,*S*,*S*)-**24** (dotted blue), **26** (gray), and (*S*,*S*,*S*,*S*,*S*,*S*,*S*)-**19** (blue), and CD spectra of (*S*,*S*,*S*,*S*,*S*,*S*,*S*)-**19** (blue). (d) UV−visible spectra of the major isomer of hexadecamer **20** (blue), **26** (gray), and hexadecamer **25** (major isomer of homocoupling of (*S*,*S*,*S*,*S*,*S*,*S*,*S*)-**9a**) (dotted blue), and CD spectra of the hexadecamer **20** (blue). Conditions: for UV spectra, chloroform, 2.0 × 10$^{-6}$ M, light pass length = 10 mm, 25 °C; for CD spectra, chloroform, 1.0 × 10$^{-4}$ M, light pass length = 1 mm, 25 °C.

field shift should be (*R*,*R*,*R*,*S*,*R*,*R*,*R*,*R*)-**31**. This technique was not applied to a series of oligonaphthalenes with ester side chains due to the small magnitude of the lower magnetic shifts of the $^{13}$C-methyl groups. Currently, the absolute configuration of **8d** was determined solely on the basis of the deference of amplitude in the CD spectrum of the homochiral isomer (major isomer,

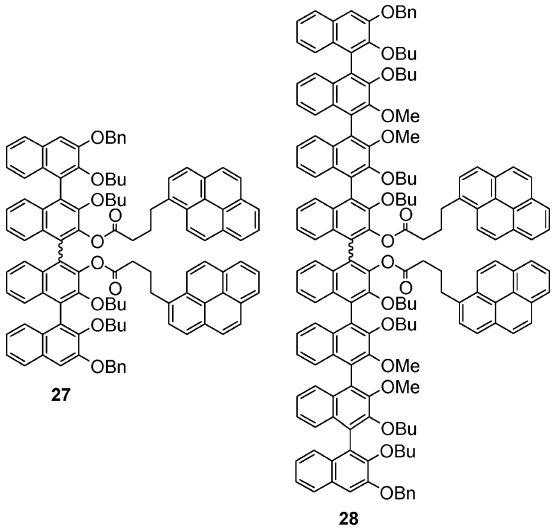


**FIGURE 9.**

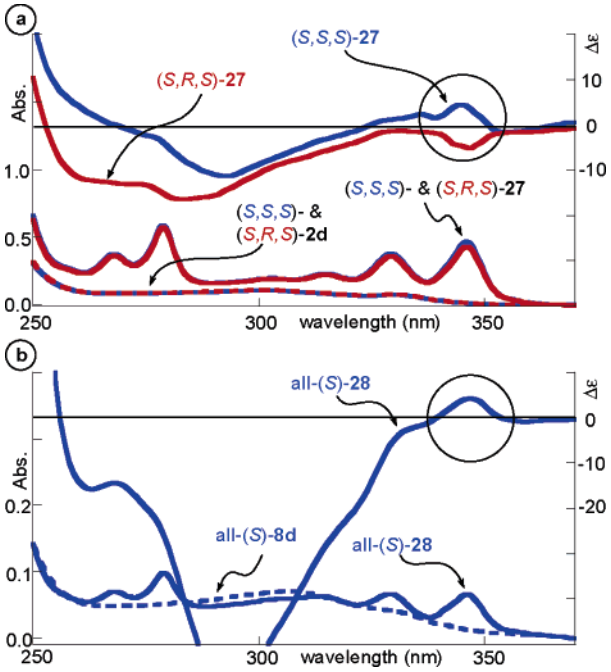


**FIGURE 10.** (a) UV−visible spectra of (*S*,*S*,*S*)-**2d** (dotted blue), (*S*,*R*,*S*)-**2d** (dotted red), (*S*,*S*,*S*)-**27** (blue), and (*S*,*R*,*S*)-**27** (red), and CD spectra of (*S*,*S*,*S*)-**27** (blue) and (*S*,*R*,*S*)-**27** (red). Conditions: for UV spectra, chloroform, $1.0 \times 10^{-5}$ M, light pass length = 10 mm, 25 °C; for CD spectra, chloroform, $1.0 \times 10^{-4}$ M, light pass length = 1 mm, 25 °C. (b) UV−visible spectra of (*S*,*S*,*S*,*S*,*S*,*S*,*S*)-**8d** (dotted blue), (*S*,*S*,*S*,*S*,*S*,*S*,*S*)-**28** (blue), and CD spectra of (*S*,*S*,*S*,*S*,*S*,*S*,*S*)-**28** (blue). Conditions: for UV spectra, chloroform, $1.0 \times 10^{-5}$ M, light pass length = 1 mm, 25 °C; for CD spectra, chloroform, $1.0 \times 10^{-5}$ M, light pass length = 1 mm, 25 °C.

*S*,*S*,*S*,*S*,*S*,*S*,*S*) and the heterochiral isomer (minor isomer, *S*,*S*,*S*,*R*,*S*,*S*,*S*).

## Conclusion

In conclusion, the syntheses for a number of optically active oligonaphthalene derivatives were developed through three different pathways, which controlled the axial chirality. The side chains on the naphthalene played crucial roles for chirality induction. To the best of our knowledge, they are the only method for constructing oligonaphthalenes where all-axial chirality, the types, and the alignments of the functional groups on the side chains were controlled. These molecules can contribute to the field of material chemistry because a versatile method for oligonaphthalenes with any number of naphthalene rings and any kind of side chains remains to be developed.

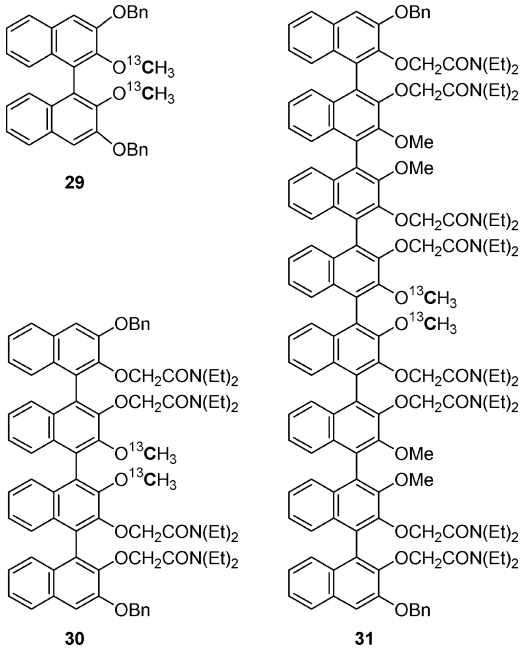


**FIGURE 11.**

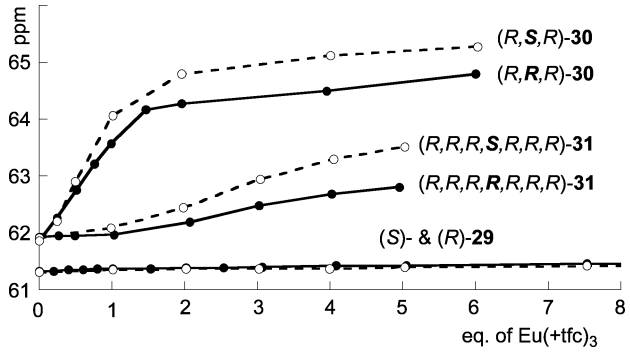


**FIGURE 12.** Conditions: concentration 10 mg/mL, $CDCl_3$, 20 °C, 50 MHz.

## Experimental Section

**General Procedure for the Synthesis of Compounds 2b−d.** The synthesis of (*R*,*R*,*R*)- and (*R*,*S*,*R*)-**2b** is typical. To a mixture of $CuCl_2$ (540 mg, 4.0 mmol) in methanol (10 mL) was added (DL)-α-phenylethylamine (0.64 mL, 5.0 mmol) under argon atmosphere under ice-bath cooling. After 30 min, a solution of (*R*)-**1b** (1.27 g, 2.0 mmol) in dichloromethane (10 mL) was added, and the reaction mixture was stirred for 2 days at 0 °C. The reaction mixture was poured into the mixed solvent of 1 M hydrochloric acid solution and ethyl acetate. The organic layer was washed with water (three times) and brine, dried over sodium sulfate, and evaporated to give a residue. The residue was purified by column chromatography ($SiO_2$, *n*-hexane/chloroform/ethyl acetate = 8/3/1) to afford (*R*,*R*,*R*)-**2b** (605 mg, 48%) and (*R*,*S*,*R*)-**2b** (69 mg, 5.4%).

**(*R*,*R*,*R*)-2b.** Colorless foam. $[\alpha]^{20}_D = +51.0$ ($c = 0.94$, $CHCl_3$). IR (KBr): 3310, 2980, 1728, 1418, 1369, 1234 $cm^{-1}$. $^1H$ NMR

(200 MHz, $CDCl_3$): $\delta$ 1.28 (s, 18H), 1.39 (s, 18H), 4.03 (d, $J$ = 16.6, 2H), 4.25 (d, $J$ = 16.6, 2H), 4.27 (d, $J$ = 15.8, 2H), 4.67 (d, $J$ = 15.8, 2H), 5.37 (s, 4H), 7.0−7.6 (m, 26H), 7.80 (d, $J$ = 8.0, 2H), 8.82 (s, 2H). HRMS (FAB) calcd for $C_{78}H_{78}O_{16}$: 1270.5290. Found: 1270.5297. Anal. Calcd for $C_{78}H_{78}O_{16}\cdot 1H_2O$: C, 72.65; H, 6.25. Found: C, 72.58; H, 6.04.

**(*R*,*S*,*R*)-2b.** Colorless foam. $[\alpha]^{20}_D = +12.8$ ($c$ = 1.00, $CHCl_3$). IR (KBr): 3454, 2979, 1750, 1726, 1439, 1369, 1234 $cm^{-1}$. $^1H$ NMR (200 MHz, $CDCl_3$): $\delta$ 1.28 (s, 18H), 1.38 (s, 18H), 4.21 (d, $J$ = 16.6, 2H), 4.23 (d, $J$ = 15.2, 2H), 4.49 (d, $J$ = 16.6, 2H), 4.70 (d, $J$ = 15.2, 2H), 5.37 (s, 4H), 7.0−7.6 (m, 26H), 7.80 (d, $J$ = 8.2, 2H), 8.71 (s, 2H). HRMS (FAB) calcd for $C_{78}H_{78}O_{16}$: 1270.5290. Found: 1270.5302. Anal. Calcd for $C_{78}H_{78}O_{16}\cdot 0.5H_2O$: C, 73.16; H, 6.22. Found: C, 73.24; H, 6.29.

**General Procedure for the Synthesis of Pyrene Compounds.** The synthesis of (*S*,*S*,*S*)-**27** is typical. To a solution of (*S*,*S*,*S*)-**2d** (25 mg, 0.024 mmol), 1-pyrenebutyric acid (21 mg, 0.072 mmol), and DMAP (3 mg) in DMF (4.0 mL) was added WSC·HCl (14 mg, 0.072 mmol), and the solution was stirred for 1 day at rt. The reaction mixture was poured into chloroform and 0.1 M hydrochloric acid. The organic layer was separated, washed successively with water (twice) and brine, dried over sodium sulfate, and evaporated in vacuo. The residue was purified by PTLC (*n*-hexane/ethyl acetate = 3/1) to afford (*S*,*S*,*S*)-**27** (34 mg, 92%). Mp 87 °C. $[\alpha]^{21}_D = -33.6$ ($c$ = 0.80, $CHCl_3$). IR (KBr): 3009, 1761, 1442, 1376 $cm^{-1}$. $^1H$ NMR (200 MHz, $CDCl_3$): $\delta$ 0.38 (t, $J$ = 7.4 Hz, 6H), 0.72 (t, $J$ = 7.4 Hz, 6H), 0.6−1.6 (m, 16H), 1.9−2.2 (m, 4H), 2.4−2.6 (m, 4H), 2.9−3.3 (m, 4H), 3.4−3.6 (m, 2H), 3.7−4.0 (m, 4H), 4.1−4.3 (m, 2H), 5.35 (s, 4H), 6.77 (t, $J$ = 7.0 Hz, 2H), 7.10−7.65 (m, 26H), 7.7−8.2 (m, 18H). HRMS (FAB) calcd for $C_{110}H_{98}O_{10}$: 1578.7160. Found: 1578.7177.

**Acknowledgment.** This paper is dedicated to the memory of the late Professor Kiyoshi Tanaka. This study was partly supported by Grants-in-Aid for Scientific Research (17659004) and the 21st Century COE Program on Kyoto University Alliance for Chemistry from the Ministry of Education, Culture, Sports, Science, and Technology, Japan.

**Supporting Information Available:** CD and UV spectra of **22**−**25**, full experimental details and characterization data of all new compounds, and crystallographic information file (CIF) of (*S*,*S*,*S*)-**2d** (CCDC 606842). This material is available free of charge via the Internet at http://pubs.acs.org.

JO060974V